

## Article

# Photocatalytic Treatment of Emerging Contaminants with Ag-Modified Titania—Is There a Risk Arising from the Degradation Products?

Robert Frankowski , Agnieszka Zgoła-Grzeskowiak \* , Tomasz Grzeskowiak , Ewa Stanisław , Justyna Werner   
and Julia Płatkiewicz 

Institute of Chemistry and Technical Electrochemistry, Poznan University of Technology, Berdychowo 4,  
60-965 Poznań, Poland

\* Correspondence: agnieszka.zgola-grzeskowiak@put.poznan.pl

**Abstract:** Bisphenol A, bisphenol S, and fluconazole are environmental contaminants widely found in surface waters because of their extensive usage and low biodegradability. Therefore, other methods are often considered for the removal of these compounds. The present study aims at their photodegradation with the use of UV light and three different catalysts, ZnO, TiO<sub>2</sub>, and Ag-TiO<sub>2</sub>. The results obtained show that photocatalytic removal of these compounds is also problematic and the use of catalysts, such as ZnO and TiO<sub>2</sub>, at increasing concentrations mostly leads to lower degradation of the tested compounds. The modification of TiO<sub>2</sub> with silver increases the degradation of both bisphenols up to 100%, which was achieved in 60 min by bisphenol A and in as little as 10 min by bisphenol S. Nevertheless, the degradation of fluconazole remained at the same level, not exceeding 70% in 60 min, i.e., still much lower than expected. In addition, the degradation products of bisphenols show the hydroxylation and destruction of their phenolic rings, while no degradation products were found during the test with fluconazole. Although the potentially genotoxic bisphenol A degradation product was found, the acute toxicity of the formed compounds differs little in comparison to the parent bisphenols.

**Keywords:** photodegradation; photocatalysis; bisphenol A; bisphenol S; fluconazole



**Citation:** Frankowski, R.; Zgoła-Grzeskowiak, A.; Grzeskowiak, T.; Stanisław, E.; Werner, J.; Płatkiewicz, J. Photocatalytic Treatment of Emerging Contaminants with Ag-Modified Titania—Is There a Risk Arising from the Degradation Products?. *Processes* **2022**, *10*, 2523. <https://doi.org/10.3390/pr10122523>

Academic Editors: Gujie Qian, Yan Zhou and Weifeng Chen

Received: 28 October 2022

Accepted: 23 November 2022

Published: 28 November 2022

**Publisher's Note:** MDPI stays neutral with regard to jurisdictional claims in published maps and institutional affiliations.



**Copyright:** © 2022 by the authors. Licensee MDPI, Basel, Switzerland. This article is an open access article distributed under the terms and conditions of the Creative Commons Attribution (CC BY) license (<https://creativecommons.org/licenses/by/4.0/>).

## 1. Introduction

Water pollution is an object of deep global concern. Water contaminated by human activities cannot be applied for household, industrial and agricultural purposes. Unfortunately, the growing population and rapid economic development worsen the situation. Therefore, the treatment of wastewater has attracted great interest, particularly the degradation of various organic pollutants using economic and pro-ecological approaches [1,2].

Among aquatic environment pollutants, azoles and bisphenols are perceived as contaminants of emerging concern [3,4]. This category of substances includes any chemical detected in the environment that cannot be monitored easily but can cause known or suspected adverse ecological or human health effects. Therefore, these compounds are not yet regulated by national and international regulations and are often found in the environment. In general, contaminants of emerging concern include many different classes of chemical compounds which can be harmful to living organisms. For example, this group can include persistent organic pollutants, brominated flame retardants, disinfection by-products, pharmaceuticals, personal care products, as well as endocrine-disrupting compounds (EDCs) [5–7], to which azoles and bisphenols belong. Endocrine disruptors can bind to the body's endocrine receptors to activate, block, or alter natural hormone synthesis. Thus, different mechanisms result in a “false” lack of or abnormal hormonal signals that increase or inhibit normal endocrine function [8,9].

Azole compounds, classified into triazoles and imidazoles, are widely used as fungicides in agriculture, human and veterinary pharmaceuticals, and personal care products due to their appreciated antifungal properties [10]. The activity of these substances is related to the possible inhibition of cytochrome P-450 enzyme activity affecting sterol biosynthesis. Thus, it decreases the ergosterol in the fungal cell membrane to alter membrane functions and permeability [11,12]. Among azole fungicides, imidazole fungicide, climbazole, and triazole fungicide, fluconazole (FLC), are very often utilized [13]. After application, the compounds are discharged along with domestic wastewater into sewage treatment plants. As traditional biochemical treatment cannot wholly remove azoles, they can enter the aquatic environment as treated wastewater and be released into the environment by irrigation and the land use of sludge [14]. The aqueous removal rates of FLC, for example, are in the range of 10–70% in studies published so far [10,15,16].

Apart from azoles, bisphenols (BPs) are also considered as endocrine disruptors. These organic compounds are a group of synthetic phenol derivatives containing two phenols connected by a linking group and are mainly utilized in the manufacturing of different types of polymers. In the group of BPs, bisphenol A (BPA), F (BPF), S (BPS), AF (BPAF), AP, B, P, Z, E, and C can be listed. Among them, BPA is the most commonly used [17]. BPs are found in many everyday products, such as cosmetics, shampoos, foods, and others, but are not used as formulation ingredients. A significant source of BPs in consumer-related products is recycled paper, cardboard, and paper used in food packaging [18,19]. Thus, the presence of BPs in the environment and many consumer products could be due to migration from the polymer and paper packaging, or the degradation of BP-containing components, representing a risk to human health [20–22].

Despite the high health risk associated with BP use, only BPA has been banned in cosmetics products to date [21]. As concerns about utilizing this bisphenol continue to grow, other compounds from this group, such as BPF and BPS, are replacing BPA in many fields. BPS often takes the place of BPA in the production of polymers that are applied in consumer products, including microwave dishes, baby bottles, artificial organs, coatings, dialyzers, thermal paper, and others [17,23–25].

Complex structures and toxicity make compounds from the group of EDCs resistant to microbial activity. They are hardly removed in conventional water or wastewater treatment processes. Thus, many EDCs and their transformation products are present in the effluents of treatment systems [5,26–28].

Due to the difficulty in removing azole fungicides and bisphenols, more effective procedures in this field are necessary [10]. Advanced oxidation processes (AOPs) have been presented as technologies capable of the degradation of some EDCs [29,30]. In general, AOPs occur in the aqueous phase with highly reactive species such as  $\text{OH}\bullet$  (hydroxyl radicals). These radicals are produced using hydrogen peroxide or a combination of UV irradiation with ozone and/or catalysts [31,32]. Hydroxyl radicals react readily with organic compounds due to the unpaired electron, significantly improving the degradation of contaminants. In general, there are no resulting products that must be removed from the effluent in the process. Thus, operational costs are reduced significantly [30,33].

Several AOP technologies are well-developed, while others are more innovative, such as Fenton's reaction and photocatalysis. In this field, photocatalytic degradation using a combination of UV irradiation with metal oxide nanostructured materials presents a promising approach that increases the number of radicals generated in the system [2]. The photocatalysts used for this purpose absorb the photons with energy equal to or greater than the bandgap energy between the valence and conduction bands of the material. As a result, the charge separation by the electrons moving from the valence to the conduction band is observed, followed by the generation of positive holes in the valence band [34]. The water is oxidized by the positive holes with the formation of large amounts of  $\text{OH}\bullet$ . At the same time, excited electrons reduce the adsorbed oxygen on the photocatalyst in the conduction band. The efficiency of photocatalytic degradation is influenced by several factors, such as the nature of organic pollutants and photocatalysts, the type of light source

and its intensity, the pH and temperature of the reaction solution, the presence of additional reagents, and others [2,35,36].

So far, a wide range of metal oxide nanomaterials ( $\text{TiO}_2$ ,  $\text{ZnO}$ ,  $\text{Fe}_2\text{O}_3$ ,  $\text{SnO}_2$ ,  $\text{WO}_3$ ,  $\text{ZrO}_2$ ,  $\text{SnO}_2$ , and others) have been tested for the photocatalytic degradation of organic pollutants into nontoxic products [2,37–39]. This study presents the development of the application of metal oxides nanoparticles ( $\text{ZnO}$ ,  $\text{TiO}_2$ , and  $\text{Ag-TiO}_2$ ) for photocatalytic degradation of FLC and two widely used bisphenols in wastewater remediation.

## 2. Materials and Methods

### 2.1. Reagents and Materials

Standards of bisphenol A, bisphenol S, and fluconazole, purchased from Sigma-Aldrich (St. Louis, MO, USA), all had a purity of at least 99%. Methanol of gradient grade purity was purchased from Merck (Darmstadt, Germany) and used for liquid chromatography. HPLC-grade water was prepared by reverse osmosis in a Demiwa system from Watek (Ledec nad Sazavou, Czech Republic), followed by double distillation from a quartz apparatus.

$\text{ZnO}$ ,  $\text{TiO}_2$ , and  $\text{Ag-TiO}_2$  were used as catalysts in the photocatalytic process.  $\text{ZnO}$  nanopowder (>97%, Aldrich, Germany) was characterized by spherical particles below 50 nm in size and with a surface area greater than  $10.8 \text{ m}^2 \text{ g}^{-1}$ .  $\text{TiO}_2$  (P25 aeroxide,  $\geq 99.5\%$ , Degussa, Germany) was characterized by spherical particles (10–30 nm) with an average particle size of ca. 21 nm, a specific surface area of  $50 \pm 15 \text{ m}^2 \text{ g}^{-1}$ , and with an anatase:rutile ratio of about 80:20. The size of the band gap was 3.05 eV for rutile and 3.20 eV for anatase.  $\text{Ag-TiO}_2$  was synthesized as described below using formic acid (89–91%, GR), NaOH (30%, Suprapur), and silver nitrate (Extra pure), which were all purchased from Merck.

### 2.2. Instrumentation

In the course of the photocatalytic degradation of model emerging contaminants, as well as the preparation of  $\text{Ag-TiO}_2$ , a cylindrical glass photoreactor (Heraeus, Hanau, Germany) was used. For photodegradation processes, the solution in the reactor was irradiated with a medium-pressure mercury vapor lamp Heraeus TQ 150 (150 W, Heraeus) fixed in a water-cooled jacket and positioned axially at the center of the reactor. The reaction temperature was kept at  $25^\circ\text{C}$  by cooling water.

For the preparation of nano- $\text{Ag-TiO}_2$ , an UV low-pressure immersion lamp TNN 15/32 (15 W, Heraeus) was utilized, which provided light with a wavelength of mainly about 254 nm. The lamp operated with a vertically arranged immersion tube immersed in the reaction liquid. The reactor was placed on top of a magnetic stirrer for agitation.

The chromatographic system from Dionex (Sunnyvale, CA, USA) consisted of a P580 A LPG gradient pump, an ASI-100 autosampler, and an STH 585 oven. A UV-VIS 170S detector and an RF 2000 fluorescence detector were used for the determination of BPA, BPS, and FLC. Identification of degradation products formed in the tests was achieved using a high-performance liquid chromatography-tandem mass spectrometry system consisting of an UltiMate 3000 HPLC from Dionex linked to a 4000 QTRAP mass spectrometer (ABSciex, Foster City, CA, USA).

The surface and morphologies of the prepared materials ( $\text{TiO}_2$  and  $\text{Ag-doped TiO}_2$  particles) were observed by scanning electron microscopy (SEM, S-3400N, Hitachi, Japan). For better image quality, the surface of non-conductive samples before analysis was coated with carbon material using a Cressington Carbon Coater. Technical data of the scanning electron microscope: cathode—tungsten wire as a source of the primary electron beam; acceleration voltage—0.3 to 30 kV; magnification—5 to  $300,000\times$  (the quality of the image at the maximum value strongly depends on many various factors); resolution—3.0 nm for a secondary electron image (30 kV acceleration voltage, in high vacuum mode), 10 nm for a secondary electron image (3 kV acceleration voltage, in high vacuum mode), 4.0 nm for a backscattered electron image (30 kV acceleration voltage, in low vacuum mode). Thermo Scientific NSS spectral imaging systems (coupled with SEM) were used for qualitative and

quantitative elemental analysis of samples using the energy dispersive X-ray spectrometry technique (EDS).

### 2.3. Preparation of the Ag-TiO<sub>2</sub> Photocatalyst

The method of preparation of the Ag-TiO<sub>2</sub> material has been described in the literature [40,41]; therefore, it will be presented here only in brief. The Ag-TiO<sub>2</sub> particles were prepared by the photoreduction of Ag(I) ions to metallic Ag on the TiO<sub>2</sub> surface. Two grams of TiO<sub>2</sub> were added to 0.5 L of deionized water in the photoreactor, followed by the addition of an aliquot of Ag(I) ions, prepared by dissolving silver nitrate in deionized water. The concentration of ions was 1% in relation to TiO<sub>2</sub>. Formic acid was adjusted to 0.025 mol L<sup>-1</sup> as carbon and used as the organic hole scavenger. The suspension was adjusted to pH 3.5 using 30% sodium hydroxide, and then irradiated for 40 min with continuous nitrogen purging. The suspension was then filtered, washed, dried, and hand-ground to obtain brown Ag-deposited TiO<sub>2</sub> particles.

### 2.4. Experimental Procedure of Photocatalytic Degradation

To investigate the removal efficiency of the model contaminants, the oxidative photodegradation of BPA, BPS, and FLC was carried out in the ZnO, TiO<sub>2</sub>, and Ag-TiO<sub>2</sub> suspensions under UV irradiation. BPA, BPS, and FLC solutions were prepared by dissolving 10 mg of solids in 1 L of water, and 650 mL of the resulting solutions were poured into the UV reactor. Appropriate amounts of catalysts were then added to the reactor to form suspensions with concentrations of oxides ranging from 0.01 to 1.0 g L<sup>-1</sup>. Prior to the photoreaction, the suspension was magnetically stirred in dark conditions for 30 min to establish an adsorption/desorption equilibrium condition (time 0 min). The aqueous suspension containing contaminant and photocatalyst was irradiated under UV light. At the given time intervals, analytical samples were taken from the suspension and immediately filtered through 0.2 µm PTFE syringe filters to remove solid particles. The filtrate was diluted and analyzed to determine the degree of degradation.

### 2.5. Analytical Method for the Determination of Tested Contaminants and Identification of Their Degradation Products

BPA, BPS, and FLC were determined in aqueous samples after photocatalytic degradation using the HPLC system described above. Further, 5 µL, 10 µL, and 20 µL samples containing BPA, BPS, and FLC, respectively, were injected into the Inertsil ODS-SP column (250 mm × 4.6 mm I.D.; 5 µm) from GL Sciences (Tokyo, Japan) maintained at 35 °C. The mobile phase consisted of 88% methanol (for the determination of BPA), 64% methanol (for the determination of BPS), and 52% methanol (for the determination of FLC) at a flow rate of 1.0 mL min<sup>-1</sup>. Signal responses were measured by fluorescence detection with wavelengths set at 273 nm for excitation and 300 nm for emission for BPA, and by UV detection with wavelengths set at 260 nm for BPS and 202 nm for FLC.

The degradation products formed in the tests were identified using the LC-MS/MS system described in Section 2.2. The samples were injected into a Kinetex Evo C18 column (150 mm × 2.1 mm I.D.; 2.6 µm) from Phenomenex (Torrance, CA, USA) maintained at 35 °C. The mobile phase (5 mM ammonium acetate in water and acetonitrile (ACN)) was used at a flow rate of 0.3 mL min<sup>-1</sup> in the following gradient: 0 min 20% ACN, 1 min 20% ACN, 5 min 100% ACN, 7 min 100% ACN. The eluate from the column was directed to the ESI source operating in positive ionization mode. The source and mass spectrometer parameters were as follows: source temperature of 450 °C, source voltage of 4500 V, nebulizer gas nitrogen at 40 psi, curtain gas nitrogen at 10 psi, auxiliary gas nitrogen at 45 psi, declustering potential of 50 V, collision gas nitrogen at 6 psi. Mass spectra were recorded in the 50–400 *m/z* range. For selected ions, chromatograms and their fragmentations were recorded in the enhanced ion product mode.

## 2.6. Toxicity Evaluation

Toxicity evaluation of bisphenols and their degradation products was performed using the ECOSAR ver. 2.0 application developed by the United States Environmental Protection Agency. The program estimates acute toxicity to fish (96 h LC50), daphnid (48 h LC50), and green algae (96 h EC50) based on the chemical structures of the compounds.

## 3. Results

### 3.1. Characterization of Synthesized Ag-TiO<sub>2</sub>

The commercially available TiO<sub>2</sub> used in the experiment was composed of 10–30 nm spherical particles and an anatase:rutile ratio of about 80:20, as described in the experimental section. As the deposition of silver was the only modification undertaken for commercial TiO<sub>2</sub>, only SEM and EDS tests were performed to compare the bare and Ag-modified materials. The SEM micrograph of TiO<sub>2</sub> particles is presented in Figure 1A. From this image, it can be observed that the material has a spongy and porous structure with sorption capabilities. On the other hand, the porous surface of the catalyst doped with Ag (Figure 1B) contains spherical structures of silver particles that appear to be stuck to the TiO<sub>2</sub> structure. EDS analysis was performed on the surface of the tested materials. This analysis confirms the presence of silver on the newly synthesized material, in contrast to the unmodified TiO<sub>2</sub>, where the presence of silver was not detected.

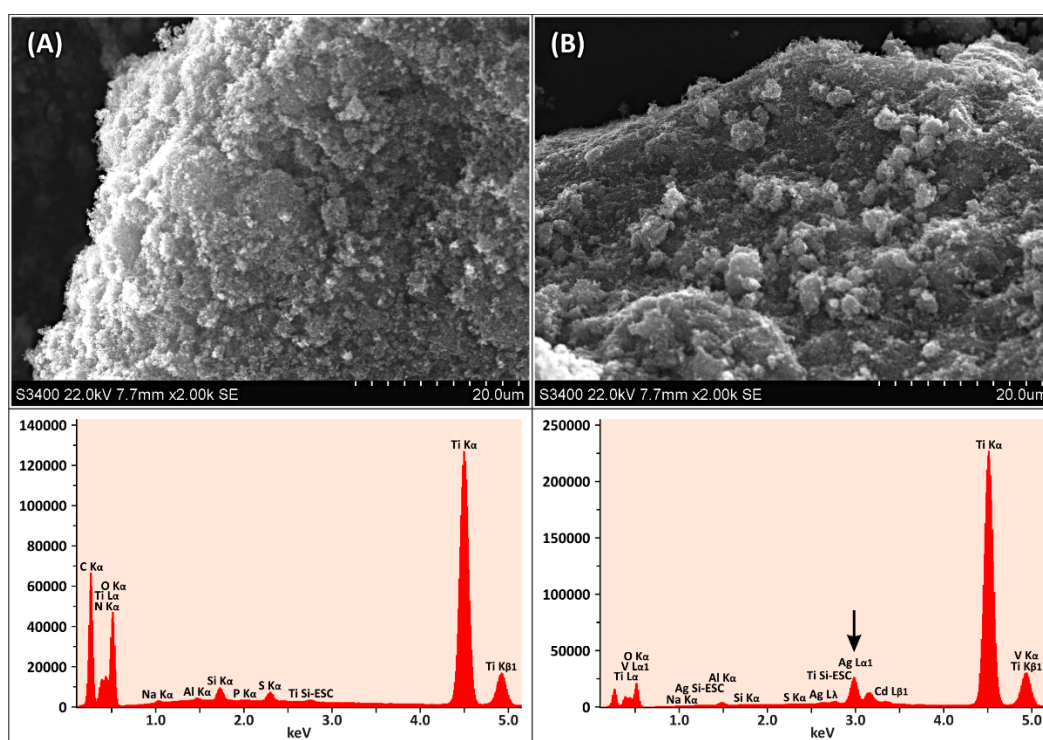


**Figure 1.** SEM micrograph and EDS analysis results of (A) TiO<sub>2</sub> and (B) Ag-doped TiO<sub>2</sub> particles.

### 3.2. Degradation Tests

Before testing the degradation of BPA, BPS, and FLC, experiments were performed to verify whether any adsorption of these compounds on ZnO, TiO<sub>2</sub>, and Ag-TiO<sub>2</sub> catalysts can be observed. The tests were performed in the dark, to eliminate the influence of light, using the oxides at a concentration equal to 0.1 g L<sup>-1</sup>. The results obtained show no substantial adsorption for BPS, as it does not exceed 5% in 60 min. The adsorption for BPA and FLC, on the other hand, reaches around 10–12% by the end of the experiments. For these two compounds, a 30-min adsorption period was added before undertaking photodegradation tests, but this step was not necessary for BPS due to the low adsorption on all three oxides.

### 3.2.1. Tests with ZnO

BPA, BPS, and FLC were subjected to photodegradation tests with a ZnO photocatalyst. Different amounts of the catalyst were used to examine whether there is an influence on the degradation rate of the tested compounds. The results presented in Figure 2 show that the amount of ZnO added does indeed matter, but the effect differs for the tested compounds. For BPA (Figure 2A), the addition of ZnO considerably decreased photodegradation. For greater concentrations of ZnO, smaller photodegradation was observed. Even at the lowest concentration of  $0.01 \text{ g L}^{-1}$ , photodegradation under UV light decreased from 90% to 70%. The addition of more ZnO resulted in a further decrease in degradation down to 40% for  $0.5 \text{ g L}^{-1}$ .

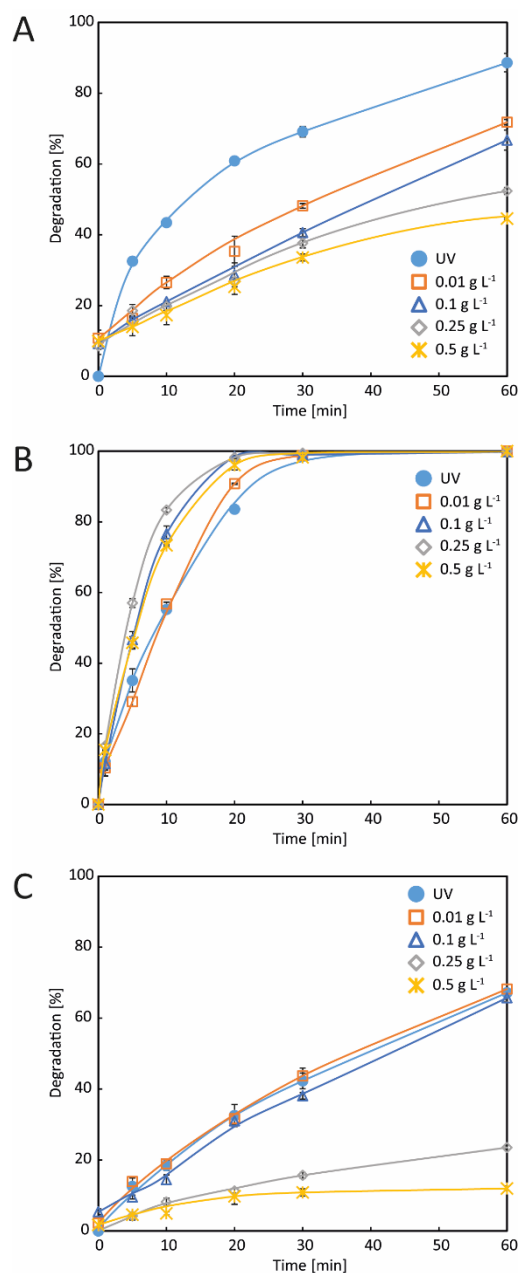


**Figure 2.** Removal of the tested compounds during photodegradation with ZnO. (A) Degradation of BPA, (B) degradation of BPS, (C) degradation of FLC. The initial concentrations of BPA, BPS, and FLC were  $10 \text{ mg L}^{-1}$ .

In contrast, the photodegradation of BPS was increased by the addition of ZnO (Figure 2B). At a concentration of  $0.01 \text{ g L}^{-1}$ , the increase was minimal, but at greater concentrations, from  $0.1 \text{ g L}^{-1}$  to  $0.5 \text{ g L}^{-1}$ , complete degradation of BPS was achieved about 10 min faster than when only UV radiation was used.

The photodegradation of FLC was the lowest among the tested compounds (Figure 2C). After 60 min of UV irradiation, less than 70% of FLC was degraded. The addition of ZnO at  $0.01 \text{ g L}^{-1}$  had no influence on the process, and at  $0.1 \text{ g L}^{-1}$ , a slight decrease was observed. However, a further increase in ZnO concentration resulted in a considerable drop in FLC degradation. For  $0.5 \text{ g L}^{-1}$  of ZnO, only 10% of FLC was removed, which equals the level observed during the adsorption tests, indicating that there was no degradation of FLC at this concentration of ZnO.

### 3.2.2. Tests with $\text{TiO}_2$

The degradation of BPA, BPS, and FLC with the  $\text{TiO}_2$  photocatalyst resulted in a similar outcome to that obtained in the presence of ZnO. The photodegradation of BPA in the presence of  $\text{TiO}_2$  decreased as the concentration of the photocatalyst increased (Figure 3A). Nevertheless, at  $0.01 \text{ g L}^{-1}$ , photodegradation was greater than when only UV irradiation was used. In addition, a slightly better removal of BPS was observed when the lowest concentration of  $\text{TiO}_2$  was used, compared to the sole use of UV irradiation (Figure 3B). A rapid decrease of degradation was observed starting from  $0.25 \text{ g L}^{-1}$ , and at  $1.0 \text{ g L}^{-1}$  only about 25% BPS was removed after 60 min. Similarly, the degradation of FLC also decreased considerably with the increasing concentration of  $\text{TiO}_2$  (Figure 3C). The effect was even worse than that observed for ZnO. A considerable 30% drop in degradation at 60 min was found even at  $0.1 \text{ g L}^{-1}$   $\text{TiO}_2$ . Further addition of  $\text{TiO}_2$  resulted in the removal of FLC equal to that observed in the adsorption tests.

### 3.2.3. Tests with $\text{Ag-TiO}_2$

The results obtained during the degradation tests of BPA, BPS, and FLC with the  $\text{Ag-TiO}_2$  photocatalyst were much different from those presented for the use of ZnO and  $\text{TiO}_2$  photocatalysts. The addition of  $\text{Ag-TiO}_2$  photocatalyst resulted in greater degradation of BPA than was observed for UV irradiation without the catalyst (Figure 4A). At  $0.01 \text{ g L}^{-1}$ , only slightly greater degradation was observed, but at higher concentrations ( $0.1\text{--}0.25 \text{ g L}^{-1}$ ), the increase was substantial. Similarly for BPS, an increase in photodegradation was also found after the addition of  $\text{Ag-TiO}_2$ , and the best results were also noted for the highest concentrations of  $\text{Ag-TiO}_2$ , while only a small increase was found at  $0.01 \text{ g L}^{-1}$  (Figure 4B). On the other hand, there was no increase or decrease in the degradation efficiency for FLC (Figure 4C). Nevertheless, the effect of using  $\text{Ag-TiO}_2$  is still much better than those noted for the ZnO and  $\text{TiO}_2$  catalysts resulting in a decrease in the degradation efficiency. Thus, even though the degradation of FLC only slightly exceeded 60%, the usage of the  $\text{Ag-TiO}_2$  catalyst is still advantageous over the application of ZnO and  $\text{TiO}_2$ . As presented in the comparison of the best degradation conditions found for each catalyst in the present study,  $\text{Ag-TiO}_2$  is the most effective catalyst for the degradation of BPA and BPS, while not decreasing the degradation of FLC (Figure 5).

## 3.3. Degradation Products and Their Toxicity

Since the most advantageous conditions of the degradation process were observed using the  $\text{Ag-TiO}_2$  photocatalyst, a more comprehensive study was undertaken to identify the degradation products formed in that process. The products found during the test with BPA included compounds formed by the attack of  $\text{OH}\bullet$  radicals on the phenolic rings, and subsequent reactions leading to the formation of quinones and the breakage of the phenolic rings (Figure 6). Further degradation of these products led to changes in the side chain formed during ring breakage. The formation of phenol was also confirmed.

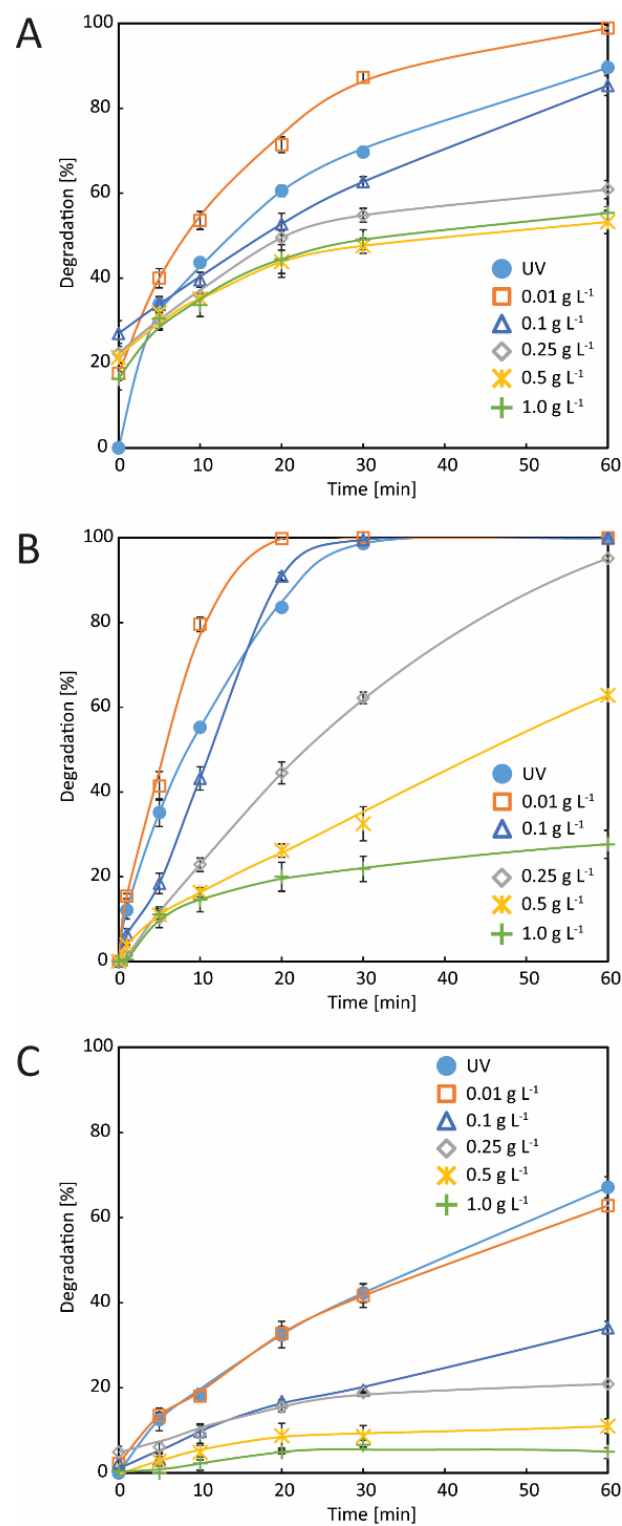


**Figure 3.** Removal of tested compounds during photodegradation with  $\text{TiO}_2$ . (A) Degradation of BPA, (B) degradation of BPS, (C) degradation of FLC. The initial concentrations of BPA, BPS, and FLC were  $10 \text{ mg L}^{-1}$ .

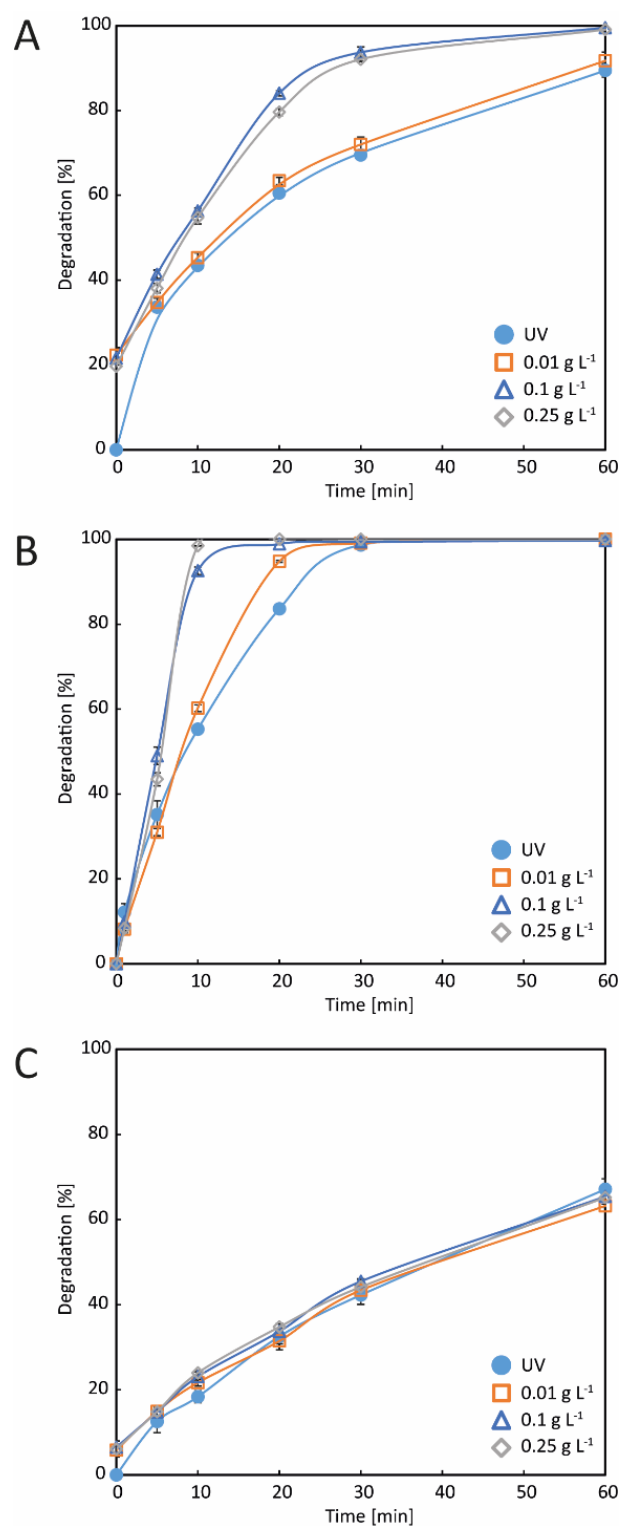


**Figure 4.** Removal of tested compounds during photodegradation with Ag-TiO<sub>2</sub>. (A) Degradation of BPA, (B) degradation of BPS, (C) degradation of FLC. The initial concentrations of BPA, BPS, and FLC were 10 mg L<sup>-1</sup>.

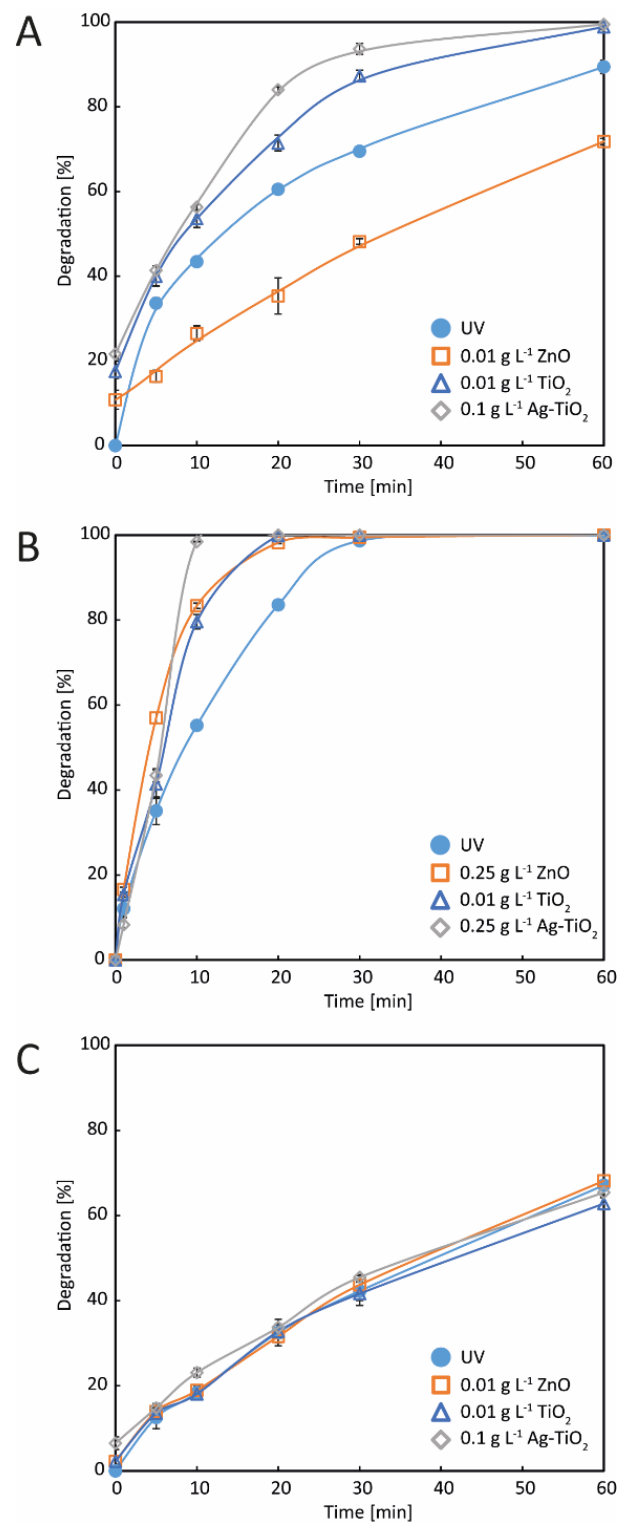


**Figure 5.** Comparison of the best degradation results obtained with the addition of three catalysts. (A) Degradation of BPA, (B) degradation of BPS, (C) degradation of FLC. The initial concentrations of BPA, BPS, and FLC were 10 mg L<sup>-1</sup>.

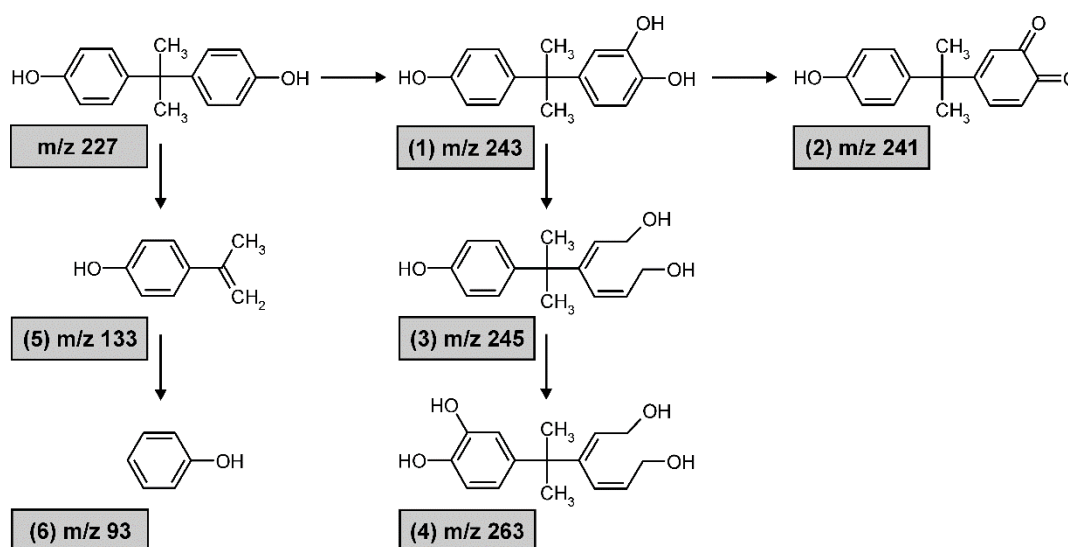


**Figure 6.** BPA and degradation products identified in its Ag-TiO<sub>2</sub>-supported photodegradation.

The photodegradation of BPS resulted in the formation of only two degradation products, phenol and sulfates, and further degradation of phenol was not observed. No degradation product formed during the photodegradation of FLC was identified due to its relatively low removal rate.

The toxicity of the tested bisphenols and their degradation products was estimated based on the calculations performed using the ECOSAR application. The acute toxicity was evaluated at three trophic levels: fish, daphnid, and green algae. For fish, the LC<sub>50</sub> value was calculated, indicating the concentration of chemicals that cause 50% death after 96 h, while for daphnids, the LC<sub>50</sub> at 48 h was estimated. On the other hand, for green algae, the EC<sub>50</sub> value was calculated, showing the concentration resulting in a 50% reduction of growth after 96 h. The results showing estimated toxicity values are presented in Table 1.

**Table 1.** Acute toxicity of bisphenols and their degradation products to fish, daphnid, and green algae.

Compound	Acute Toxicity to Fish, LC <sub>50</sub> at 96 h (mg mL <sup>-1</sup> )	Acute Toxicity to Daphnid, LC <sub>50</sub> at 96 h (mg mL <sup>-1</sup> )	Acute Toxicity to Green Algae, LC <sub>50</sub> at 96 h (mg mL <sup>-1</sup> )
BPA	1.28	5.24	1.33
(1)	2.65	13.1	2.07
(2)	4.15	3.25	0.38
(3)	2.45	5.72	0.13
(4)	3.59	8.88	0.23
(5)	3.99	2.67	0.36
(6)	27.7	9.64	2.40
BPS	21.8	196	6.90

## 4. Discussion

### 4.1. Removal of Tested Compounds during the Degradation

ZnO and TiO<sub>2</sub>-based catalysts are often used in the photodegradation of different pollutants [42–44] and are often tested for use in the degradation of BPA, a widely utilized endocrine-disrupting compound often found in the environment [45–47]. ZnO has been used for the degradation of BPA, both in its native form [48,49] and when doped with various elements [50,51]. Compared to the present study, where photocatalysis with ZnO resulted in 70% degradation of BPA in one hour, An et al. [48] achieved a 70–90% removal of BPA during the same time and, contrary to the present study, slightly better degradation

was achieved at greater concentrations of ZnO. Zacharakis et al. [49] immobilized ZnO on a glass plate to test the degradation of BPA at a thousand-times-lower concentration, and also observed up to 80% of its removal. Using carbon and cerium-doped ZnO, Bechambi et al. [50,51] achieved a removal of BPA of about 30%, and discovered that applying concentrations of doped ZnO that were too high resulted in a lowering of the degradation of BPA; however, this effect was observed at concentrations ZnO greater than those in the present study.

No literature reports were found on the degradation of BPS and FLC in the presence of ZnO. However, the degradation of other azoles has been reported, including metronidazole, which was degraded up to almost 60% in one hour with ZnO catalyst [52], similar to FLC degradation in the present study. Two other azoles were tested using a 1:1 mixture of ZnO:TiO<sub>2</sub>, and the authors reported a half-life (removal of 50%) for bifonazole and clotrimazole as long as 16 and 7 h, respectively [53,54]. Nevertheless, any degradation results obtained for other azoles would be difficult to interpret due to the differences in structures compared to FLC (in analogy to the difference in degradation noted in the present study for BPA and BPS).

The degradation of BPA using TiO<sub>2</sub> has been examined in many laboratories and many modifications of this catalyst have been tested to achieve a better removal the BPA compound. Tsai et al. [55] tested the removal of BPA with UV radiation and TiO<sub>2</sub> catalyst under different experimental conditions. Contrary to the present study, the authors observed faster degradation with increasing load of the catalyst—no light absorption or scattering caused by the catalyst was found. Zacharakis et al. [49] immobilized TiO<sub>2</sub> and found a similar dependence, i.e., faster degradation with more TiO<sub>2</sub> in the system. On the other hand, to prevent such effects, Lee et al. [56] tested TiO<sub>2</sub> catalyst immobilized on glass tubes in the photodegradation of BPA, achieving its removal within a few hours. Although the degradation time was a few times longer than in the present study, immobilization made the catalyst reusable without problems connected with recycling TiO<sub>2</sub> from treated wastewater, in the case of future large-scale applications. In the study presented by An et al. [48], there was no considerable difference in the removal of BPA depending on TiO<sub>2</sub> concentration. This comparison shows that the experimental conditions tested in various laboratories, even though apparently similar, may result in different outcomes. Thus, the usage of TiO<sub>2</sub> in the commercial treatment of wastewater may be difficult to optimize due to many changes in the incoming sewage. Modifications of the TiO<sub>2</sub> catalyst were also tested for the removal of BPA. For example, Yu et al. [57] modified TiO<sub>2</sub> with graphene oxide, where the tested graphene-modified TiO<sub>2</sub> photocatalyst enabled a relatively fast removal of BPA under UV irradiation within half an hour from turning the UV light on, i.e., twice faster than the unmodified TiO<sub>2</sub> used in the present study.

Although TiO<sub>2</sub> and modified TiO<sub>2</sub> are often tested for the removal of BPA, these photocatalysts are rarely used for the degradation of other bisphenols and azoles. Jia et al. [58] experimented with the TiO<sub>2</sub> photocatalytic activation of peroxymonosulfate for the removal of three bisphenols: BPS, BPF, and BPAF. Out of the three tested bisphenols, the lowest degradation was found for BPS, achieving about 70% in one hour. In the present study under optimized conditions, BPS was removed in 20 min. TiO<sub>2</sub> was also used in the removal of fluconazole. Sousa et al. [59] tested the TiO<sub>2</sub>-assisted photocatalytic degradation of emerging contaminants in the effluent of a municipal wastewater treatment plant. The presented results show poor degradability of fluconazole, similar to those obtained in our laboratory.

The modification of TiO<sub>2</sub> with noble metals improves the electron-hole separation, due to the attraction of electrons by these metals, and promotes oxidation [60,61]. As a result, Ag-TiO<sub>2</sub> improves the degradation of many compounds, including BPA [60,62]. An improvement in the removal of BPA and BPS was also noted in the present study. For both BPA and BPS, faster degradation was observed at increasing concentrations of Ag-TiO<sub>2</sub> photocatalyst. At the highest concentration of the catalyst tested (0.25 g L<sup>-1</sup>), BPA was removed in one hour and BPS in 10 min. In contrast, there was no effect of the removal of

FLC, which showed neither an increase nor a decrease. This, however, is better than the decrease noted upon the addition of ZnO or unmodified TiO<sub>2</sub>.

The phenomenon of decreased degradations obtained for both ZnO and TiO<sub>2</sub> after the addition of the catalyst (Figures 2 and 3) may be caused by both light absorption and diffusion, due to the presence of the catalysts suspended in the solution. Apparently, the capability of ZnO and TiO<sub>2</sub> to support the degradation is much lower than the loss of efficiency caused by lower irradiation reaching the tested compounds. Therefore, the surface degradation cannot be calculated as the difference between the total degradation and the bulk solution degradation observed in the test using UV irradiation only. Interestingly, no such phenomenon was observed for Ag-TiO<sub>2</sub> (Figure 4). Even the smallest addition of this catalyst induces more degradation compared to the reduction in the bulk solution degradation caused by its presence. Nevertheless, it must be taken into account that even for Ag-TiO<sub>2</sub>, the surface degradation and the bulk degradation observed in the test using UV irradiation only may also not be additive.

It is also interesting to note that for FLC, no effect of Ag-TiO<sub>2</sub> addition was observed. Although no reduction was caused by its presence, no increase was also found. This may be due to the molecule of FLC containing several nitrogen atoms with free electron pairs repelling the radicals formed in the photocatalytic process. Further studies may be needed to achieve better degradation of FLC.

#### 4.2. Comparison with Other Studies

Studies on the photocatalytic removal of BPA were conducted by different researchers. Among the tested catalysts, ZnO, TiO<sub>2</sub>, and Ag-TiO<sub>2</sub> were also used. Table 2 lists several examples of photocatalytic degradation of pollutants (mainly BPA, due to its wide usage), showing the degradation efficiency of the methods using these catalysts. As can be found in Table 2, photodegradation in the presence of ZnO, even supported by the addition of H<sub>2</sub>O<sub>2</sub>, resulted in lower degradation compared to that found for Ag-TiO<sub>2</sub> in the present study. TiO<sub>2</sub> was also used with H<sub>2</sub>O<sub>2</sub>, resulting in a 100% removal of BPA in 1 h, but without H<sub>2</sub>O<sub>2</sub>, a low removal of BPA was found. Similarly, the photodegradation of BPS was also satisfactory when TiO<sub>2</sub> was used with the addition of KHSO<sub>5</sub> as the oxidizing agent. On the other hand, the use of Ag-TiO<sub>2</sub> was successful in the removal of BPA, except for the study by Shareef et al. [62], who used a catalyst-coated ceramic membrane which possibly blocked the UV irradiation from reaching the catalyst. Unfortunately, the degradation of fluconazole by similar catalysts has not been found in the literature.

**Table 2.** Degradation of BPA, BPS, and FLC under different experimental conditions reported in the literature.

Pollutant/Concentration, mg L <sup>-1</sup>	Photocatalyst/Additive/pH	Degradation Efficiency in 1 h (%)	Ref.
BPA/100	ZnO/H <sub>2</sub> O <sub>2</sub> /6.3	90	[48]
BPA/0.1	ZnO/H <sub>2</sub> O <sub>2</sub> /-	85	[49]
BPA/50	ZnO (C-doped)/H <sub>2</sub> O <sub>2</sub> /8–9	70	[50]
BPA/50	ZnO (Ce-doped)/H <sub>2</sub> O <sub>2</sub> /9	60	[51]
BPA/20	TiO <sub>2</sub> /H <sub>2</sub> O <sub>2</sub> /5–9	100	[55]
BPA/10	TiO <sub>2</sub> /-/3	15	[56]
BPS/10	TiO <sub>2</sub> /KHSO <sub>5</sub> /3	95	[58]
BPA/10	Ag-TiO <sub>2</sub> /-/5.3	100	[60]
BPA/10	Ag-TiO <sub>2</sub> /-/	35	[62]
BPA/10	Ag-TiO <sub>2</sub> /-/	100	Present study
BPS/10	Ag-TiO <sub>2</sub> /-/	100 (in 10 min)	Present study
FLC/10	Ag-TiO <sub>2</sub> /-/	60	Present study

#### 4.3. Formation of the Degradation Products and Their Toxicity

Under the conditions applied in the photodegradation using the Ag-TiO<sub>2</sub> photocatalyst, the products formed in the degradation of BPA included those created by the attack of

OH• radicals to the phenolic rings and those formed after BPA scission (Figure 6). Among the compounds created in the first path, both BPA-catechol (1) and BPA-quinone (2) were found. The formation of these compounds was reported in other studies on the oxidative degradation of BPA. Kondrakov et al. [63] tested photocatalysis with TiO<sub>2</sub> and found both compounds (1) and (2). The same compounds were also observed in our previous study on the photo-Fenton reaction [64]. Mehrabani-Zeinabad et al. [65] revealed the formation of (1) during advanced oxidation of BPA (including ozonation, photooxidation, and photooxidation in the presence of hydrogen peroxide), and compound (2) was reported by Kuvuran and Yildirim [66] in their studies on the ozonation of BPA. Compound (3) has not been reported, but its further degradation to diacid can be expected, as reported by Kuvuran and Yildirim [66]. In addition, compounds formed by the oxidation of two phenolic rings that may be precursors of compound (4) were reported by Kondrakov et al. [63].

The second degradation path involved BPA scission and led to the formation of isopropenephenol (5) and traces of phenol (6). Compound (5) and other products of BPA scission were found by Hua et al. [67] in heterogeneous Fenton degradation. Other scission products, including both (5) and (6), were reported by Bechambi et al. [50] in photocatalytic degradation with ZnO. Figure 7 shows the formation and decay of the degradation products. It can be seen that compound (5) is both created and removed very quickly, while the products formed by the attack of OH• radicals on the phenolic rings appear more slowly and can be found even after 90 min of the photodegradation process.

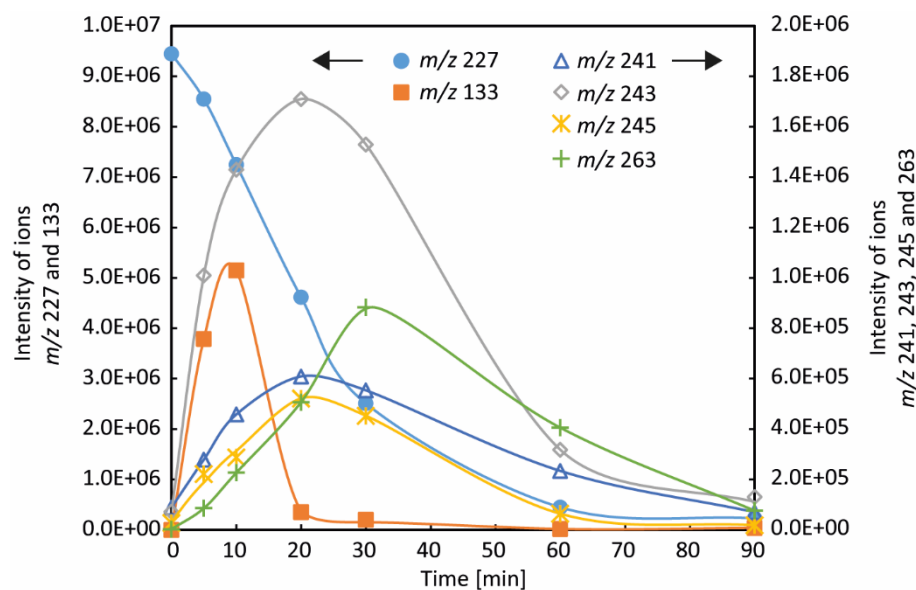


**Figure 7.** Formation and decay of compounds found during the photodegradation of BPA.

Among the numerous degradation products identified in the present study, compound (2) deserves special attention because it may be genotoxic [63] and has been reported in three studies [63,64,66]. Therefore, it is very important to achieve a fast degradation of BPA to remove not only the parent compound, but also the vast majority of its degradation products. However, in many studies on BPA oxidation, including the present one, BPA degradation is very slow. Figure 7 shows that compound (2) is formed at the very beginning of the oxidation process and can be found even after 90 min. Although its accumulation is not observed, its slow decay during 90 min of the process is an undesirable phenomenon. Therefore, BPA should be degraded during another oxidation process, or subjected to preliminary biodegradation to avoid the release of compound (2) into the environment.

The proposed photodegradation of BPS resulted in the formation of phenol and sulfates. The compounds were also found in our previous study on BPS removal by the photo-Fenton reaction [64]. The presence of phenol was reported by Mehrabani-Zeinabad et al. [65] during different degradation tests of BPS (ozonation and photooxidation in

the presence of ozone or hydrogen peroxide). Additionally, the formation of  $\text{SO}_3$  in the photooxidation process with hydrogen peroxide was demonstrated by the same authors.

As presented in Table 1, the acute toxicity of all identified BPA degradation products to fish is lower than that of BPA. The toxicity to daphnid is lower than that of BPA for most identified compounds, and greater only in the case of (2) and (5). On the other hand, only two degradation compounds, (1) and (6), have a lower toxicity to green algae, while all the others are more toxic. Nevertheless, the differences in toxicity of BPA and its degradation compounds estimated for all three organisms is very low; it is not greater than about ten times for green algae. For BPS, a comparison could be made only with phenol (compound (6) in Table 1), and it shows a similar acute toxicity of these two compounds to fish. For both daphnid and green algae, the toxicity of phenol emerging in the degradation process is only three to twenty times greater than that of BPS.

## 5. Conclusions

The efficiency of the photocatalytic process with UV irradiation strongly depends on the amount of catalyst added. However, the effect differs for the examined compounds. For a greater concentration of ZnO, a smaller photodegradation of BPA was observed. On the contrary, the photodegradation of BPS was increased by the addition of ZnO. The photodegradation of FLC with ZnO was the lowest among the tested compounds. After 60 min of UV irradiation, less than 70% of FLC was degraded, and the addition of ZnO did not improve the process. The degradation of BPA, BPS, and FLC with the  $\text{TiO}_2$  photocatalyst resulted in a similar outcome to that obtained in the presence of ZnO. The addition of  $\text{TiO}_2$  increased the degradation of BPA and BPS only at the lowest concentration, while greater amounts of these two catalysts decreased the degradation of these bisphenols considerably. No influence on FLC was noted using the smallest addition of  $\text{TiO}_2$ , and degradation decreased considerably after the addition of greater amounts of the catalyst.

The results obtained during the degradation tests of BPA, BPS, and FLC with Ag- $\text{TiO}_2$  photocatalyst were much different from those presented for the use of ZnO and  $\text{TiO}_2$ . The effect of Ag- $\text{TiO}_2$  on degradation efficiency is much better than those noted for the ZnO and  $\text{TiO}_2$  catalysts. Application of the Ag- $\text{TiO}_2$  catalysts is beneficial, as in the tested concentration range, it never adversely affected the degradation of tested compounds. Moreover, although the degradation of FLC was not increased and only slightly exceeded 60%, the application of the Ag- $\text{TiO}_2$  catalyst is more advantageous over ZnO and  $\text{TiO}_2$ , because no decrease in degradation was observed for this compound also.

The degradation of both bisphenols during photocatalysis with Ag- $\text{TiO}_2$  was attained relatively fast. There were two types of degradation products found in the degradation of BPA: those resulting from the breakage of the alkyl chain and those from the oxidation of the phenol rings. The products of alkyl chain breakage were removed very fast, while those arising from ring oxidation remained longer, including BPA-quinone that may be genotoxic. On the other hand, degradation products of BPS contained only those resulting from its oxidative breakage, that is, phenol and sulfates. However, although degradation caused great structural changes in both bisphenols, the acute toxicity estimated for bisphenols and their degradation products showed little difference.

**Author Contributions:** Conceptualization, R.F., A.Z.-G. and T.G.; methodology, R.F., A.Z.-G. and T.G.; validation, R.F., A.Z.-G. and T.G.; investigation, R.F., A.Z.-G., E.S., J.W. and J.P.; writing—original draft preparation, R.F., A.Z.-G., T.G., E.S. and J.W.; writing—review and editing, R.F., A.Z.-G., T.G. and E.S.; visualization, R.F. and A.Z.-G.; supervision, A.Z.-G.; project administration, A.Z.-G.; funding acquisition, A.Z.-G. All authors have read and agreed to the published version of the manuscript.

**Funding:** This research was funded by the Polish Ministry of Education and Science, grant number 0911/SBAD/2206.

**Data Availability Statement:** The data that support the findings of this study are available from the corresponding author upon request.

**Conflicts of Interest:** The authors declare no conflict of interest.

## References

1. Pignatello, J.J.; Oliveros, E.; MacKay, A. Advanced oxidation processes for organic contaminant destruction based on the Fenton reaction and related chemistry. *Crit. Rev. Environ. Sci. Technol.* **2006**, *36*, 1–84. [[CrossRef](#)]
2. Gusain, R.; Gupta, K.; Joshi, P.; Khatri, O.P. Adsorptive removal and photocatalytic degradation of organic pollutants using metal oxides and their composites: A comprehensive review. *Adv. Colloid Interface Sci.* **2019**, *272*, 102009. [[CrossRef](#)] [[PubMed](#)]
3. Patel, N.; Khan, M.D.; Shahane, S.; Rai, D.; Chauhan, D.; Kant, C.; Chaudhary, V.K. Emerging pollutants in aquatic environment: Source, effect, and challenges in biomonitoring and bioremediation—A review. *Pollution* **2020**, *6*, 99–113. [[CrossRef](#)]
4. Pironti, C.; Ricciardi, M.; Proto, A.; Bianco, P.M.; Montano, L.; Motta, O. Endocrine-disrupting compounds: An overview on their occurrence in the aquatic environment and human exposure. *Water* **2021**, *13*, 1347. [[CrossRef](#)]
5. Petrie, B.; Barden, R.; Kasprzyk-Hordern, B. A review on emerging contaminants in wastewater and the environment: Current knowledge, understudied areas and recommendations for future monitoring. *Water Res.* **2015**, *72*, 3–27. [[CrossRef](#)] [[PubMed](#)]
6. Wang, H.; Xi, H.; Xu, L.; Jin, M.; Zhao, W.; Liu, H. Ecotoxicological effects, environmental fate and risks of pharmaceutical and personal care products in the water environment: A review. *Sci. Total Environ.* **2021**, *788*, 147819. [[CrossRef](#)] [[PubMed](#)]
7. Ahmad, A.; Kurniawan, S.B.; Abdullah, S.R.S.; Othman, A.R.; Hasan, H.A. Contaminants of emerging concern (CECs) in aquaculture effluent: Insight into breeding and rearing activities, alarming impacts, regulations, performance of wastewater treatment unit and future approaches. *Chemosphere* **2022**, *290*, 133319. [[CrossRef](#)] [[PubMed](#)]
8. Sharma, V.K.; Anquandah, G.A.K.; Nesnas, N. Kinetics of the oxidation of endocrine disruptor nonylphenol by ferrate(VI). *Environ. Chem. Lett.* **2009**, *7*, 115–119. [[CrossRef](#)]
9. Zoeller, R.T.; Brown, T.R.; Doan, L.L.; Gore, A.C.; Skakkebaek, N.E.; Soto, A.M.; Woodruff, T.J.; Vom Saal, F.S. Endocrine-disrupting chemicals and public health protection: A statement of principles from The Endocrine Society. *Endocrinology* **2012**, *153*, 4097–4110. [[CrossRef](#)] [[PubMed](#)]
10. Kahle, M.; Buerge, I.J.; Hauser, A.; Müller, M.D.; Poiger, T. Azole fungicides: Occurrence and fate in wastewater and surface waters. *Environ. Sci. Technol.* **2008**, *42*, 7193–7200. [[CrossRef](#)] [[PubMed](#)]
11. Joseph-Horne, T.; Hollomon, D.W. Molecular mechanisms of azole resistance in fungi. *FEMS Microbiol. Lett.* **1997**, *149*, 41–149. [[CrossRef](#)] [[PubMed](#)]
12. Georgopadakou, N.H. Antifungals: Mechanism of action and resistance, established and novel drugs. *Curr. Opin. Microbiol.* **1998**, *1*, 547–557. [[CrossRef](#)]
13. Cai, W.; Ye, P.; Yang, B.; Shi, Z.; Xiong, Q.; Gao, F.; Liu, J.; Zhao, J.; Ying, G. Biodegradation of typical azole fungicides in activated sludge under aerobic conditions. *J. Environ. Sci.* **2021**, *103*, 288–297. [[CrossRef](#)] [[PubMed](#)]
14. Peschka, M.; Roberts, P.H.; Knepper, T.P. Analysis, fate studies and monitoring of the antifungal agent clotrimazole in the aquatic environment. *Anal. Bioanal. Chem.* **2007**, *389*, 959–968. [[CrossRef](#)] [[PubMed](#)]
15. Peng, X.; Huang, Q.; Zhang, K.; Yu, Y.; Wang, Z.; Wang, C. Distribution, behavior and fate of azole antifungals during mechanical, biological, and chemical treatments in sewage treatment plants in China. *Sci. Total Environ.* **2012**, *426*, 311–317. [[CrossRef](#)] [[PubMed](#)]
16. Chen, Z.-F.; Ying, G.-G. Occurrence, fate and ecological risk of five typical azole fungicides as therapeutic and personal care products in the environment: A review. *Environ. Int.* **2015**, *84*, 142–153. [[CrossRef](#)] [[PubMed](#)]
17. Hu, Y.; Zhu, Q.; Yan, X.; Liao, C.; Jiang, G. Occurrence, fate and risk assessment of BPA and its substituents in wastewater treatment plant: A review. *Environ. Res.* **2019**, *178*, 108732. [[CrossRef](#)] [[PubMed](#)]
18. Liao, C.; Kannan, K. Widespread occurrence of bisphenol A in paper and paper products: Implications for human exposure. *Environ. Sci. Technol.* **2011**, *45*, 9372–9379. [[CrossRef](#)] [[PubMed](#)]
19. Wu, L.H.; Zhang, X.M.; Wang, F.; Gao, C.J.; Chen, D.; Palumbo, J.R.; Guo, Y.; Zeng, E.Y. Occurrence of bisphenol S in the environment and implications for human exposure: A short review. *Sci. Total Environ.* **2018**, *615*, 87–98. [[CrossRef](#)]
20. Cacho, J.I.; Campillo, N.; Viñas, P.; Hernández-Córdoba, M. Stir bar sorptive extraction with EG-Silicone coating for bisphenols determination in personal care products by GC-MS. *J. Pharmaceut. Biomed. Anal.* **2013**, *78–79*, 255–260. [[CrossRef](#)]
21. Martín-Pozo, L.; del Carmen Gómez-Regalado, M.; Moscoso-Ruiz, I.; Zafra-Gómez, A. Analytical methods for the determination of endocrine disrupting chemicals in cosmetics and personal care products: A review. *Talanta* **2021**, *234*, 122642. [[CrossRef](#)] [[PubMed](#)]
22. Lestido-Cardama, A.; Millán Sánchez, B.; Sendón, R.; Rodríguez-Bernaldo de Quirós, A.; Barbosa-Pereira, L. Study on the chemical behaviour of bisphenol S during the in vitro gastrointestinal digestion and its bioaccessibility. *Food Chem.* **2021**, *367*, 130758. [[CrossRef](#)] [[PubMed](#)]
23. Chen, D.; Kannan, K.; Tan, H.; Zheng, Z.; Feng, Y.L.; Wu, Y.; Widelka, M. Bisphenol analogues other than BPA: Environmental occurrence, human exposure, and toxicity—A review. *Environ. Sci. Technol.* **2016**, *50*, 5438–5453. [[CrossRef](#)] [[PubMed](#)]
24. Noszczyńska, M.; Piotrowska-Seget, Z. Bisphenols: Application, occurrence, safety, and biodegradation mediated by bacterial communities in wastewater treatment plants and rivers. *Chemosphere* **2018**, *201*, 214–223. [[CrossRef](#)] [[PubMed](#)]
25. Frankowski, R.; Zgoła-Grześkowiak, A.; Grześkowiak, T.; Sójka, K. The presence of bisphenol A in the thermal paper in the face of changing European regulations e A comparative global research. *Environ. Pollut.* **2020**, *265*, 114879. [[CrossRef](#)] [[PubMed](#)]
26. Majumder, A.; Gupta, B.; Gupta, A.K. Pharmaceutically active compounds in aqueous environment: A status, toxicity and insights of remediation. *Environ. Res.* **2019**, *176*, 108542. [[CrossRef](#)] [[PubMed](#)]

27. Parida, V.K.; Saidulu, D.; Majumder, A.; Srivastava, A.; Gupta, B.; Gupta, A.K. Emerging contaminants in wastewater: A critical review on occurrence, existing legislations, risk assessment, and sustainable treatment alternatives. *J. Environ. Chem. Eng.* **2021**, *9*, 105966. [[CrossRef](#)]
28. Rathi, B.S.; Kumar, P.S.; Show, P.L. A review on effective removal of emerging contaminants from aquatic systems: Current trends and scope for further research. *J. Hazard. Mater.* **2021**, *409*, 124413. [[CrossRef](#)] [[PubMed](#)]
29. O'Shea, K.E.; Dionysiou, D.D. Advanced oxidation processes for water treatment. *J. Phys. Chem. Lett.* **2012**, *3*, 2112–2113. [[CrossRef](#)]
30. Fast, S.A.; Gude, V.G.; Truax, D.D.; Martin, J.; Magbanua, B.S. A critical evaluation of advanced oxidation processes for emerging contaminants removal. *Environ. Process.* **2017**, *4*, 283–302. [[CrossRef](#)]
31. Andreozzi, R.; Caprio, V.; Insola, A.; Marotta, R. Advanced oxidation processes (AOP) for water purification and recovery. *Catal. Today* **1999**, *53*, 51–59. [[CrossRef](#)]
32. Patel, M.; Kumar, R.; Kishor, K.; Mlsna, T.; Pittman, C.U.; Mohan, D. Pharmaceuticals of emerging concern in aquatic systems: Chemistry, occurrence, effects, and removal methods. *Chem. Rev.* **2019**, *119*, 3510–3673. [[CrossRef](#)] [[PubMed](#)]
33. Oturan, M.A.; Aaron, J.-J. Advanced oxidation processes in water/wastewater treatment: Principles and applications. A review. *Crit. Rev. Environ. Sci. Technol.* **2014**, *44*, 2577–2641. [[CrossRef](#)]
34. Ajith, M.P.; Aswath, M.; Priyadarshini, E.; Rajamani, P. Recent innovations of nanotechnology in water treatment: A comprehensive review. *Bioresour. Technol.* **2021**, *342*, 126000. [[CrossRef](#)] [[PubMed](#)]
35. Ahmed, S.; Rasul, M.G.; Brown, R.; Hashib, M.A. Influence of parameters on the heterogeneous photocatalytic degradation of pesticides and phenolic contaminants in wastewater: A short review. *J. Environ. Manag.* **2011**, *92*, 311–330. [[CrossRef](#)] [[PubMed](#)]
36. Rauf, M.A.; Meetani, M.A.; Hisaindee, S. An overview on the photocatalytic degradation of azo dyes in the presence of TiO<sub>2</sub> doped with selective transition metals. *Desalination* **2011**, *276*, 13–27. [[CrossRef](#)]
37. Gupta, S.M.; Tripathi, M. A review of TiO<sub>2</sub> nanoparticles. *Chin. Sci. Bull.* **2011**, *56*, 1639–1657. [[CrossRef](#)]
38. Tahir, M.B.; Nawaz, T.; Nabi, G.; Sagir, M.; Khan, M.I.; Malik, N. Role of nanophotocatalysts for the treatment of hazardous organic and inorganic pollutants in wastewater. *Int. J. of Environ. Anal. Chem.* **2022**, *102*, 491–515. [[CrossRef](#)]
39. Sun, C.; Yang, J.; Xu, M.; Cui, Y.; Ren, W.; Zhang, J.; Zhao, H.; Liang, B. Recent intensification strategies of SnO<sub>2</sub>-based photocatalysts: A review. *Chem. Eng. J.* **2022**, *427*, 131564. [[CrossRef](#)]
40. Matusiewicz, H.; Stanisiz, E. Evaluation of the catalyzed photo-cold vapour generation for determination of mercury by AAS. *J. Braz. Chem. Soc.* **2012**, *23*, 247–257. [[CrossRef](#)]
41. Tan, T.T.Y.; Yip, C.K.; Beydoun, D.; Amal, R. Effects of nano-Ag particles loading on TiO<sub>2</sub> photocatalytic reduction of selenate ions. *Chem. Eng. J.* **2003**, *95*, 179–186. [[CrossRef](#)]
42. Khaki, M.R.D.; Shafeeyan, M.S.; Raman, A.A.A.; Daud, W.M.A.W. Application of doped photocatalysts for organic pollutant degradation—A review. *J. Environ. Manag.* **2017**, *198*, 78–94. [[CrossRef](#)] [[PubMed](#)]
43. Majumder, S.; Chatterjee, S.; Basnet, P.; Mukherjee, J. ZnO based nanomaterials for photocatalytic degradation of aqueous pharmaceutical waste solutions—A contemporary review. *Environ. Nanotechnol. Monit. Manag.* **2020**, *14*, 100386. [[CrossRef](#)]
44. Yahya, N.; Aziz, F.; Jamaludin, N.A.; Mutalib, M.A.; Ismail, A.F.; Salleh, W.N.W.; Jaafar, J.; Yusof, N.; Ludin, N.A. A review of integrated photocatalyst adsorbents for wastewater treatment. *J. Environ. Chem. Eng.* **2018**, *6*, 7411–7425. [[CrossRef](#)]
45. Abraham, A.; Chakraborty, P. A review on sources and health impacts of bisphenol A. *Rev. Environ. Health* **2020**, *35*, 201–210. [[CrossRef](#)]
46. Huang, Y.Q.; Wong, C.K.C.; Zheng, J.S.; Bouwman, H.; Barra, R.; Wahlström, B.; Neretin, L.; Wong, M.H. Bisphenol A (BPA) in China: A review of sources, environmental levels, and potential human health impacts. *Environ. Int.* **2012**, *42*, 91–99. [[CrossRef](#)]
47. Rotimi, O.A.; Olawole, T.D.; De Campos, O.C.; Adelani, I.B.; Rotimi, S.O. Bisphenol A in Africa: A review of environmental and biological levels. *Sci. Total Environ.* **2021**, *764*, 142854. [[CrossRef](#)]
48. An, S.-N.; Choi, N.-C.; Choi, J.-W.; Lee, S. Photodegradation of bisphenol A with ZnO and TiO<sub>2</sub>: Influence of metal ions and Fenton process. *Water Air Soil Pollut.* **2018**, *229*, 43. [[CrossRef](#)]
49. Zacharakis, A.; Chatzisyneon, E.; Binas, V.; Frontistis, Z.; Venieri, D.; Mantzavinos, D. Solar Photocatalytic Degradation of Bisphenol A on Immobilized ZnO or TiO<sub>2</sub>. *Int. J. Photoenergy* **2013**, *2013*, 570587. [[CrossRef](#)]
50. Bechambi, O.; Sayadi, S.; Najjar, W. Photocatalytic degradation of bisphenol A in the presence of C-doped ZnO: Effect of operational parameters and photodegradation mechanism. *J. Ind. Eng. Chem.* **2015**, *32*, 201–210. [[CrossRef](#)]
51. Bechambi, O.; Jlaiei, L.; Najjar, W.; Sayadi, S. Photocatalytic degradation of bisphenol A in the presence of Ce-ZnO: Evolution of kinetics, toxicity and photodegradation mechanism. *Mater. Chem. Phys.* **2016**, *173*, 95–105. [[CrossRef](#)]
52. Farzadkia, M.; Esrafil, A.; Baghapour, M.A.; Shahamat, Y.D.; Okhovat, N. Degradation of metronidazole in aqueous solution by nano-ZnO/UV photocatalytic process. *Desalination Water Treat.* **2014**, *52*, 4947–4952. [[CrossRef](#)]
53. Kryczyk, A.; Żmudzki, P.; Hubicka, U. Determination of bifonazole and identification of its photocatalytic degradation products using UPLC-MS/MS. *Biomed. Chromatogr.* **2017**, *31*, e3955. [[CrossRef](#)] [[PubMed](#)]
54. Kryczyk, A.; Żmudzki, P.; Koczurkiewicz, P.; Piotrowska, J.; Pękala, E.; Hubicka, U. The impact of ZnO and TiO<sub>2</sub> on the stability of clotrimazole under UVA irradiation: Identification of photocatalytic degradation products and in vitro cytotoxicity assessment. *J. Pharm. Biomed. Anal.* **2017**, *145*, 283–292. [[CrossRef](#)]
55. Tsai, W.-T.; Lee, M.-K.; Su, T.-Y.; Chang, Y.-M. Photodegradation of bisphenol-A in a batch TiO<sub>2</sub> suspension reactor. *J. Hazard. Mater.* **2009**, *168*, 269–275. [[CrossRef](#)]

56. Lee, J.-M.; Kim, M.-S.; Kim, B.-W. Photodegradation of bisphenol-A with TiO<sub>2</sub> immobilized on the glass tubes including the UV light lamps. *Water Res.* **2004**, *38*, 3605–3613. [[CrossRef](#)]
57. Yu, F.; Bai, X.; Yang, C.; Xu, L.; Ma, J. Reduced graphene oxide-P25 nanocomposites as efficient photocatalysts for degradation of bisphenol A in water. *Catalysts* **2019**, *9*, 607. [[CrossRef](#)]
58. Jia, J.; Liu, D.; Wang, Q.; Li, H.; Ni, J.; Cui, F.; Tian, J. Comparative study on bisphenols oxidation via TiO<sub>2</sub> photocatalytic activation of peroxymonosulfate: Effectiveness, mechanism and pathways. *J. Hazard. Mater.* **2022**, *424*, 127434. [[CrossRef](#)]
59. Sousa, M.A.; Gonçalves, C.; Vilar, V.J.P.; Boaventura, R.A.R.; Alpendurada, M.F. Suspended TiO<sub>2</sub>-assisted photocatalytic degradation of emerging contaminants in a municipal WWTP effluent using a solar pilot plant with CPCs. *Chem. Eng. J.* **2012**, *198–199*, 301–309. [[CrossRef](#)]
60. Rengaraj, S.; Li, X.Z. Photocatalytic degradation of bisphenol A as an endocrine disruptor in aqueous suspension using Ag-TiO<sub>2</sub> catalysts. *Int. J. Environ. Pollut.* **2006**, *27*, 20–37. [[CrossRef](#)]
61. Suwanchawalit, C.; Wongnawa, S.; Sriprang, P.; Meanha, P. Enhancement of the photocatalytic performance of Ag-modified TiO<sub>2</sub> photocatalyst under visible light. *Ceram. Int.* **2012**, *38*, 5201–5207. [[CrossRef](#)]
62. Shareef, U.; Othman, M.H.D.; Ismail, A.F.; Jilani, A. Facile removal of bisphenol A from water through novel Ag-doped TiO<sub>2</sub> photocatalytic hollow fiber ceramic membrane. *J. Aust. Ceram. Soc.* **2020**, *56*, 29–39. [[CrossRef](#)]
63. Kondrakov, A.O.; Ignatev, A.N.; Frimmel, F.H.; Bräse, S.; Horn, H.; Revelsky, A.I. Formation of genotoxic quinones during bisphenol A degradation by TiO<sub>2</sub> photocatalysis and UV photolysis: A comparative study. *Appl. Catal. B Environ.* **2014**, *160–161*, 106–114. [[CrossRef](#)]
64. Frankowski, R.; Płatkiewicz, J.; Stanisław, E.; Grzeškowiak, T.; Zgoła-Grzeškowiak, A. Biodegradation and photo-Fenton degradation of bisphenol A, bisphenol S and fluconazole in water. *Environ. Pollut.* **2021**, *289*, 117947. [[CrossRef](#)] [[PubMed](#)]
65. Mehrabani-Zeinabad, M.; Langford, C.H.; Achari, G. Advanced oxidative degradation of bisphenol A and bisphenol S. *J. Environ. Eng. Sci.* **2015**, *10*, 92–102. [[CrossRef](#)]
66. Kusvuran, E.; Yildirim, D. Degradation of bisphenol A by ozonation and determination of degradation intermediates by gas chromatography–mass spectrometry and liquid chromatography–mass spectrometry. *Chem. Eng. J.* **2013**, *220*, 6–14. [[CrossRef](#)]
67. Hua, Z.; Ma, W.; Bai, X.; Feng, R.; Yu, L.; Zhang, X.; Dai, Z. Heterogeneous Fenton degradation of bisphenol A catalyzed by efficient adsorptive Fe<sub>3</sub>O<sub>4</sub>/GO nanocomposites. *Environ. Sci. Pollut. Res.* **2014**, *21*, 7737–7745. [[CrossRef](#)]